Proceedings of the 9th World Congress on Mechanical, Chemical, and Material Engineering (MCM'23)
Brunel University, London, United Kingdom - August 06-08, 2023
Paper No. ICMIE 152
DOI: 10.11159/icmie23.152

Thermal Entrance Length for the Laminar Forced Convection in Microtubes

Mohamed Shaimi[1], Rabha Khatyr[2], Jaafar Khalid Naciri[3]
Laboratory of Mechanics, Faculty of Sciences Aïn Chock, Hassan II University of Casablanca
Km 8 Route d'El Jadida, B.P 5366 Maarif 20100, Casablanca 20000, Morocco
[1] mohamed.shaimi-etu@etu.univh2c.ma ; [2] khatyrrabha@gmail.com ; [3] naciriuh2c@gmail.com

***Abstract* -** In this paper, the thermal entrance length for the laminar forced convection in circular microtubes is investigated. The flow is considered steady incompressible and hydrodynamically developed, and the fluid Newtonian with constant thermophysical properties. The effects of viscous dissipation, axial conduction and slip flow are taken into account. The first-order slip-velocity and temperature jump models are used for the wall boundary conditions. An exact analytical solution is used to calculate for the velocity and temperature distributions. Furthermore, the Nusselt number is determined in terms of the Brinkman number, the Péclet number and the Knudsen number. The effects of the Brinkman number, Péclet number, and the Knudsen number on the thermal entrance length are presented. It is found that the thermal entrance length is approximately compared to the radius for small Péclet numbers while it is continuously increasing for large values of the Péclet number. Otherwise, the thermal entrance length decreases as the absolute value of the Brinkman number increases.

***Keywords*:** Laminar Forced Convection, Thermal Entrance Length, Brinkman Number, Péclet Number, Knudsen Number

1. Introduction

Heat transfer in the microscale is very important for the development of many industrial products such as micro heat-exchangers that are used in various applications. The forced convection, also known as the Graetz problem, is one of the fundamental topics in the study of heat transfer. Graetz was the first to study this problem in 1882 [1]. Shah and London (1978) [1] reviewed different analytical and numerical solutions to this problem using various configurations in the macroscale. Lahjomri and Oubarra (1999) [2] studied the extended Graetz problem, which includes the axial heat conduction effects, in parallel-plate channels and circular tubes. They solved the problem using an exact analytical solution. Recently, Haddout *et al.* (2020) [3] presented an analytical study of the extended Graetz problem in parallel-plate microchannels and circular microtubes in the case of a fixed characteristic mean velocity. Shaimi *et al.* (2023) [4] presented a comparative study for the extended Graetz problem in parallel-plate microchannels and circular microtubes between the case of a fixed characteristic pressure drop, which is of significant importance in optimization problems [5,6], and the fixed characteristic mean velocity, which is exhaustively studied in the literature [3]. A direct exact solution in the case of a fixed characteristic pressure drop was presented along with the relationship, between the pressure drop and the mean velocity, to be used in order to obtain the solution in the case of a fixed characteristic mean velocity.

The objective of this paper is to investigate the effects of the axial heat conduction, viscous dissipation, and slip flow on the thermal entrance length of a laminar forced convection in microtubes. The microtube is considered infinite with constant wall temperature including a step change in its value at a given abscissa. The flow is assumed to be steady incompressible and hydrodynamically developed, and the fluid is considered Newtonian with constant thermophysical properties. The wall boundary conditions are given by the first-order slip-velocity and temperature jump models. The effects of the Péclet number, Brinkman number, and Knudsen number on the thermal entrance length are presented.

This paper is divided into five sections. The analysis is presented in the second section. Then, the thermal entrance length calculation is demonstrated in the third section. After that, the results and discussions are shown in the fourth section. Finally, a conclusion is presented to summarize the current investigation.

2. Analysis

The circular microtube is axisymmetric as shown in Fig. 1. R is the radius of the microtube and (r^*, z^*) are cylindrical coordinates. The wall temperature is defined by a step function where it is given by the constant, T_0, for $z^* < 0$ and the constant, T_w, for $z^* > 0$. At $z^* = \pm\infty$, the temperature profiles are considered developed.

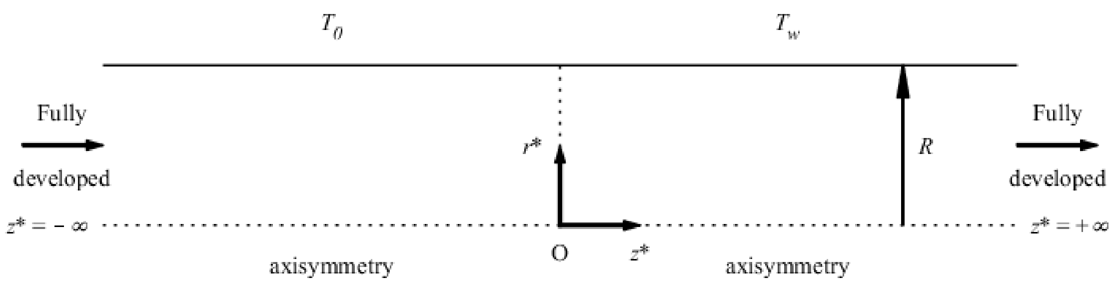

Fig. 1: The geometrical configuration of the studied microtube.

The Newtonian fluid flow is assumed to be steady, laminar, incompressible, and hydrodynamically developed. The first-order slip-velocity and temperature jump models are used for wall boundary conditions. Under these assumptions, the governing equations are given by [4]:

$$\frac{1}{r^*}\frac{d}{dr^*}\left(r^*\frac{du^*}{dr^*}\right) = \frac{1}{\mu}\frac{dp^*}{dz^*} \tag{1}$$

$$\rho C_p u^*(r^*)\frac{\partial T_j^*}{\partial z^*} = k\left(\frac{\partial^2 T_j^*}{\partial z^{*2}} + \frac{1}{r^*}\frac{\partial}{\partial r^*}\left(r^*\frac{\partial T_j^*}{\partial r^*}\right)\right) + \mu\left(\frac{du^*}{dr^*}\right)^2 \tag{2}$$

where ρ, μ, C_p, k, p^*, and u^* are respectively the density, dynamic viscosity, specific heat, thermal conductivity, pressure, and axial velocity of the fluid. T_j^* is the temperature distribution of the fluid with $j = 1$ for the upstream region $(z^* < 0)$ and $j = 2$ for the downstream region $(z^* > 0)$.

The boundary conditions are written as follows [4]:

$$\left.\frac{du^*}{dr^*}\right|_{r^*=0} = 0;\quad \left.\frac{\partial T_1^*}{\partial r^*}\right|_{r^*=0} = 0;\quad \left.\frac{\partial T_2^*}{\partial r^*}\right|_{r^*=0} = 0 \tag{3}$$

$$u^*(r^* = R) = -\frac{2-\sigma_v}{\sigma_v}\lambda\left.\frac{du^*}{dr^*}\right|_{r^*=R} \tag{4}$$

$$T_1^*(z^*, r^* = R) - T_0 = -\frac{2-\sigma_T}{\sigma_T}\frac{2\gamma}{\gamma+1}\frac{\lambda}{Pr}\left.\frac{\partial T_1^*}{\partial r^*}\right|_{r^*=R};\quad T_2^*(z^*, r^* = R) - T_w = -\frac{2-\sigma_T}{\sigma_T}\frac{2\gamma}{\gamma+1}\frac{\lambda}{Pr}\left.\frac{\partial T_2^*}{\partial r^*}\right|_{r^*=R} \tag{5}$$

$$T_1^*(z^* = 0, r^*) = T_2^*(z^* = 0, r^*) \text{ for } 0 \le r^* < R;\quad \left.\frac{\partial T_1^*}{\partial z^*}\right|_{z^*=0} = \left.\frac{\partial T_2^*}{\partial z^*}\right|_{z^*=0} \tag{6}$$

$$T_1^*(z^* = -\infty, r^*) = T_{-\infty}^*(r^*);\quad T_2^*(z^* = +\infty, r^*) = T_{+\infty}^*(r^*) \tag{7}$$

where λ, σ_v, σ_T, γ, and $Pr = \frac{\mu C_p}{k}$ are respectively the mean free path of the molecules, tangential accommodation coefficient, energy accommodation coefficient, specific heat ratio, and Prandtl number. Equation (3) represents the axisymmetry conditions. Equations (4) and (5) are respectively the slip-velocity and the temperature jump at the stationary isothermal wall. Equation (6) shows the continuity of the temperature and the axial heat flux at the junction section $(z^* = 0)$ which is the section of the step change in the wall temperature. Equation (7) represents the developed profiles of the temperature far upstream at $z^* = -\infty$ $\left(T^*_{-\infty}(r^*)\right)$ and far downstream at $z^* = +\infty$ $\left(T^*_{+\infty}(r^*)\right)$ that are to be calculated by using Eqs. (2) and (5).

The dimensionless variables are defined as follows [4] considering a fixed characteristic pressure drop:

$$z = \frac{z^*}{R \cdot Pe}; \quad r = \frac{r^*}{R}; \quad u = \frac{u^*}{\frac{R^2}{4\mu}\Delta p_L}; \quad T_j = \frac{T_j^* - T_w}{T_0 - T_w} \tag{8}$$

where $Pe = \frac{\rho C_p R^3 \Delta p_L}{4\mu k}$ is the Péclet number and $\Delta p_L = -\frac{dp^*}{dz^*}$ = constant is the pressure drop per unit length [4].

Integrating Eq. (1) and using Eqs. (3), (4), and (8) leads to the following dimensionless velocity distribution [4]:

$$u(r) = 1 - r^2 + 4\frac{2-\sigma_{\mathrm{v}}}{\sigma_{\mathrm{v}}}Kn \tag{9}$$

where $Kn = \frac{\lambda}{2R}$ is the Knudsen number.

Substituting Eq. (8) into Eq. (2) leads to the following dimensionless energy equation:

$$u(r)\frac{\partial T_j}{\partial z} = \frac{1}{Pe^2}\frac{\partial^2 T_j}{\partial z^2} + \frac{1}{r}\frac{\partial}{\partial r}\left(r\frac{\partial T_j}{\partial r}\right) + Br\left(\frac{du}{dr}\right)^2 \tag{10}$$

where $Br = \frac{R^4(\Delta p_L)^2}{16\mu k(T_0 - T_w)}$ is the Brinkman number.

The dimensionless boundary conditions become [4]:

$$\left.\frac{\partial T_1}{\partial r}\right|_{r=0} = 0; \quad \left.\frac{\partial T_2}{\partial r}\right|_{r=0} = 0 \tag{11}$$

$$T_1(z, r=1) = 1 - 2\,\kappa\,Kn\left.\frac{\partial T_1}{\partial r}\right|_{r=1}; \quad T_2(z, r=1) = -2\,\kappa\,Kn\left.\frac{\partial T_2}{\partial r}\right|_{r=1} \tag{12}$$

$$T_1(z=0, r) = T_2(z=0, r) \text{ for } 0 \le r < 1; \quad \left.\frac{\partial T_1}{\partial z}\right|_{z=0} = \left.\frac{\partial T_2}{\partial z}\right|_{z=0} \tag{13}$$

$$T_1(z=-\infty, r) = 1 + \frac{Br}{4}(1 - r^4 + 8\,\kappa\,Kn); \quad T_2(z=+\infty, r) = \frac{Br}{4}(1 - r^4 + 8\,\kappa\,Kn) \tag{14}$$

where $\kappa = \frac{2-\sigma_T}{\sigma_T}\frac{2\gamma}{\gamma+1}\frac{1}{Pr}$ is a characteristic parameter accounting for the degree of temperature jump. Equation (14) shows the expressions of the developed dimensionless temperature profiles which are obtained by integrating Eq. (10) and using Eqs. (11) and (12).

The dimensionless temperature distributions are sought in the following form [4]:

$$T_1(z, r) = 1 + \frac{Br}{4}(1 - r^4 + 8\,\kappa\,Kn) + \sum_n A_n f_n(r) e^{\alpha_n^2 z} \tag{15}$$

$$T_2(z, r) = \frac{Br}{4}(1 - r^4 + 8\,\kappa\,Kn) + \sum_n B_n g_n(r) e^{-\beta_n^2 z} \tag{16}$$

where A_n and B_n are expansion constants, α_n and β_n are real eigenvalues respectively associated with the eigenfunctions f_n and g_n that are given [4]:

$$f_n(r) = e^{-\frac{i\alpha_n r^2}{2}} M(a_n, c, i\alpha_n r^2) \tag{17}$$

$$g_n(r) = e^{-\frac{\beta_n r^2}{2}} M(b_n, c, \beta_n r^2) \tag{18}$$

where $a_n = \frac{1}{2} - \frac{i+8\frac{2-\sigma_v}{\sigma_v}Kn}{4}\alpha_n + \frac{i\alpha_n^3}{4Pe^2}$, $b_n = \frac{1}{2} - \frac{1+8\frac{2-\sigma_v}{\sigma_v}Kn}{4}\beta_n - \frac{\beta_n^3}{4Pe^2}$, $c = 1$, and M is the Kummer confluent first-kind hypergeometric function.

The eigenvalues are calculated as roots of $f_n(r=1) + 2\kappa\, Kn \frac{df_n}{dr}\Big|_{r=1} = 0$ and $g_n(r=1) + 2\kappa\, Kn \frac{dg_n}{dr}\Big|_{r=1} = 0$ which are derived from Eq. (12). The expansion constants are determined by using Eq. (13) as follows [3]:

$$A_n = \frac{2}{\alpha_n \left[\frac{df_n(r=1)}{d\alpha_n} + 2\kappa\, Kn \frac{d}{d\alpha_n}\left(\frac{df_n}{dr}\Big|_{r=1}\right)\right]} \tag{19}$$

$$B_n = -\frac{2}{\beta_n \left[\frac{dg_n(r=1)}{d\beta_n} + 2\kappa\, Kn \frac{d}{d\beta_n}\left(\frac{dg_n}{dr}\Big|_{r=1}\right)\right]} \tag{20}$$

The local Nusselt number for $z > 0$ is given by [4]:

$$Nu(z) = \frac{-2\, \frac{\partial T_2}{\partial r}\Big|_{r=1}}{T_b(z)} \tag{21}$$

where $T_b(z) = \frac{\int_0^1 u(r)\, T_2(z,r)\, r\, dr}{\int_0^1 u(r)\, r\, dr}$ is the dimensionless bulk temperature.

3. Thermal Entrance Length

The step change in the wall temperature of the microtube leads to the existence of a thermal entrance region. The inlet of this thermal entrance region is the junction section where the temperature profile is obtained by solving the energy equation in the upstream region with the associated boundary conditions. The thermal entrance region ends as the fully developed flow is achieved which is characterized by a constant Nusselt number. Therefore, the thermal entrance length is defined as the length required to achieve, to a given degree of accuracy, the constant fully developed Nusselt number. There are different reported criteria in the literature [1] that are somewhat arbitrary on how to determine the thermal entrance length. In this paper, the thermal entrance length is defined as the length required to achieve a value of the local Nusselt number Nu that satisfies $0.99 \cdot Nu_{FD} < Nu < 1.01 \cdot Nu_{FD}$ where Nu_{FD} is the fully developed Nusselt number.

In the case of a fixed characteristic pressure drop, presented in section 2, the dimensionless thermal entrance length is $z_{th} = \frac{z_{th}^*}{R \cdot Pe}$ (Eq. (8)). The mean velocity in terms of the pressure drop is given by:

$$U_m = \frac{R^2 \Delta p_L}{4\mu}\left(\frac{1}{2} + 4\frac{2-\sigma_\text{v}}{\sigma_\text{v}} Kn\right) \tag{22}$$

Otherwise, for the case of a fixed characteristic mean velocity U_m, the dimensionless variables are redefined in terms of U_m. Therefore, z, u, Pe, and Br are modified by using Eq. (22) as follows [4]:

$$Z = \frac{z}{1+8\frac{2-\sigma_v}{\sigma_v}Kn};\ U = \frac{u}{\frac{1}{2}+4\frac{2-\sigma_v}{\sigma_v}Kn};\ Pe_U = \left(1+8\frac{2-\sigma_v}{\sigma_v}Kn\right)Pe;\ Br_U = \left(\frac{1}{2}+4\frac{2-\sigma_v}{\sigma_v}Kn\right)^2 Br \tag{23}$$

where $Z = \frac{z^*}{R\,Pe_U}$, $U = \frac{u^*}{U_m}$, $Pe_U = \frac{2\rho C_p R U_m}{k}$, and $Br_U = \frac{\mu {U_m}^2}{k(T_0 - T_w)}$ are respectively the newly defined dimensionless axial coordinate, dimensionless velocity, Péclet number, and Brinkman number in terms of U_m. Let us note that in the case of $Kn = 0$, $Z = z$ and $Pe_U = Pe$ (Eq. (23)). Finally, the dimensionless thermal entrance length in the case of a fixed characteristic mean velocity is $Z_{th} = \frac{z_{th}^*}{R \cdot Pe_U}$.

The dimensionless thermal entrance lengths z_{th} and Z_{th} are defined in terms of Pe and Pe_U, which means that they are dependent on the flow through ΔP_L and U_m as well as fluid properties. Therefore, to obtain a dimensionless form of the thermal entrance length, that is purely geometrical, then the Péclet number is removed as follows:

$$L_{th} = \frac{z_{th}^*}{R} = z_{th} Pe = Z_{th} Pe_U \tag{24}$$

4. Results and Discussions

In this section, the effects of the Péclet number, Brinkman number, Knudsen number, and degree of temperature jump are presented. In the following, the pure diffuse reflection $\sigma_v = 1$ [7] is considered. Both the no-slip flow $Kn \le 10^{-3}$ and the slip flow $10^{-3} < Kn \le 0.1$ [7] are presented in what follows.

Figures 2(a)-(b) show the evolution of the thermal entrance length (respectively Z_{th} and L_{th}) as a function of the Péclet number (Pe_U) with no viscous dissipation ($Br_U = 0 \rightarrow Br = 0$) and no-slip condition ($Kn = 0$ which means that $Z_{th} = z_{th}$ and $Pe_U = Pe$). As can be seen from Fig. 2(a), Z_{th} decreases significantly as Pe_U increases for small Péclet numbers ($Pe_U < 10$) while it reaches approximately a constant value ($Z_{th} \sim 0.11$) for large Péclet numbers. Moreover, Fig. 2(b) shows that L_{th} increases continuously as Pe_U increases for large Péclet numbers. This can be argued from the dimensionless energy equation using $\xi = \frac{z^*}{R}$ and expressed for $Br = 0$ as follows:

$$Pe\, u(r)\frac{\partial T_j}{\partial \xi} = \frac{\partial^2 T_j}{\partial \xi^2} + \frac{1}{r}\frac{\partial}{\partial r}\left(r\frac{\partial T_j}{\partial r}\right) \tag{25}$$

As can be seen from Eq. (25), the convective term in the left-hand side becomes more important as the Péclet number increases which induces an increase in the thermal entrance length L_{th}. Thus, for large Péclet numbers the thermal entrance region can be large (depending on the length of the tube) while it is approximately compared to the radius ($L_{th} \sim 1.4 \cdot R$) for small Péclet numbers ($Pe_U < 10$).

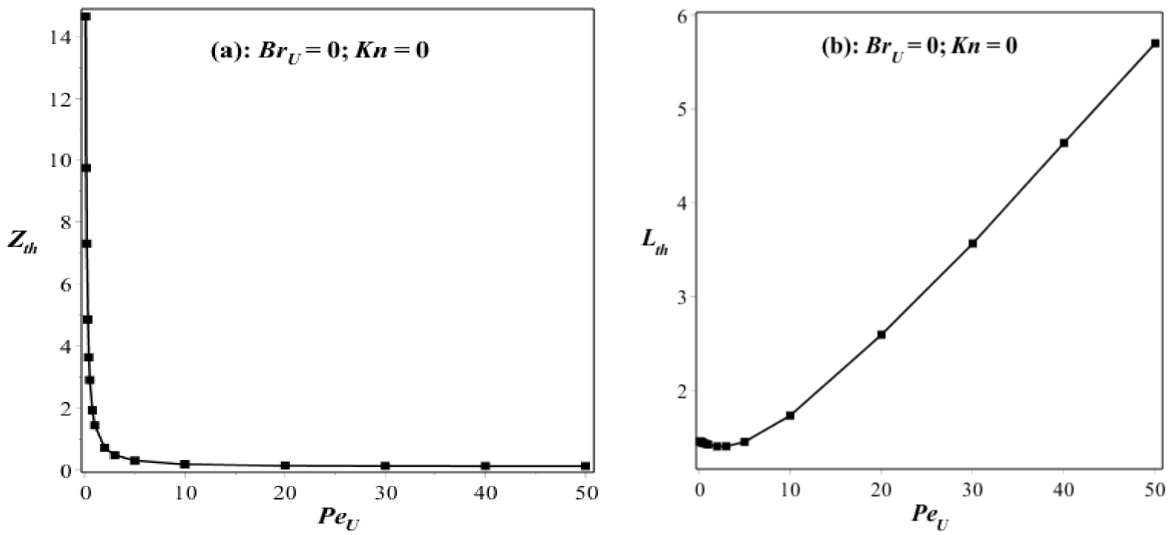

Fig. 2: Evolution of the thermal entrance length as a function of the Péclet number with no viscous dissipation and no-slip condition.

Figures 3(a)-(b) show the evolution of the thermal entrance length (respectively Z_{th} and L_{th}) as a function of the Brinkman number (Br_U) for different Péclet numbers and no-slip condition ($Kn = 0$ which means that $Z_{th} = z_{th}$ and $Pe_U = Pe$). It is found that the thermal entrance length is approximately independent of the Brinkman number's sign ($Br_U > 0$ for fluid cooling, $T_w < T_0$, and $Br_U < 0$ for fluid heating, $T_w > T_0$). Furthermore, the thermal entrance length decreases as $|Br_U|$ increases which is induced by the increase of the viscous dissipation effects. This is verified from the dimensionless energy equation (Eq. (10)) where the increase in the viscous dissipation term leads to a decrease in the convective term and consequently leads to a decrease of the thermal entrance length. Additionally, in the presence of the viscous dissipation (Fig. 3(b)), L_{th} increases as Pe_U increases similarly to the observed effect in Fig. 2(b).

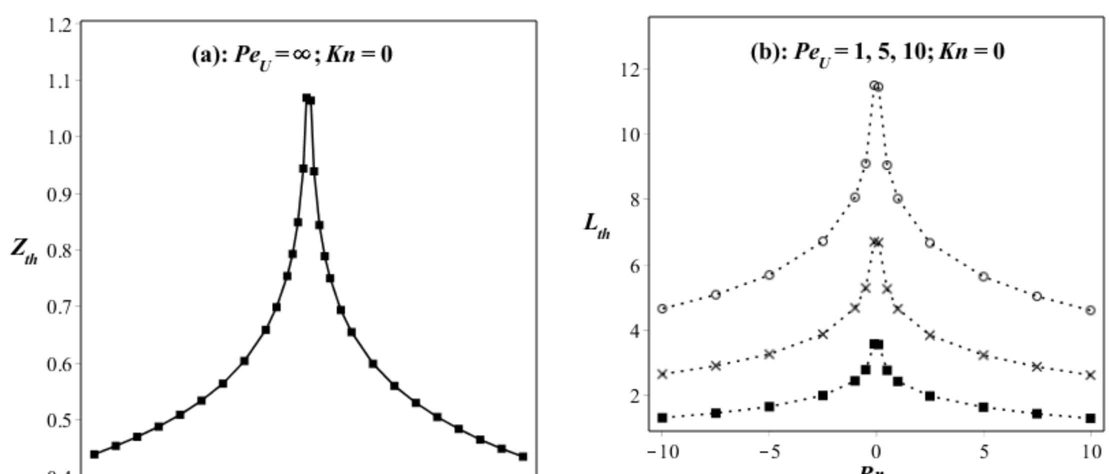

Fig. 3: Evolution of the thermal entrance length as a function of the Brinkman number for different Péclet numbers with no-slip condition.

Figure 4(a) shows the evolution of z_{th} and Z_{th} as a function of the Knudsen number for negligible axial heat conduction ($Pe_U = \infty \rightarrow Pe = \infty$) and no viscous dissipation ($Br_U = 0 \rightarrow Br = 0$) in the cases of no temperature jump condition ($\kappa = 0$) and the presence of temperature jump ($\kappa = 1.667$) including both cases of a fixed pressure drop and a fixed mean velocity. It is observed that in the case of a fixed mean velocity, Z_{th}~0.11 with slow decrease and slow increase as Kn increases respectively for no temperature jump, $\kappa = 0$, and for $\kappa = 1.667$. This is due to the fixed mean velocity which induces approximately an unchangeable convective term. In the other hand for a fixed pressure drop, z_{th} increases as Kn increases. The temperature jump increases both z_{th} and Z_{th}. This is due to the increase of the mean velocity as Kn increases for a fixed pressure drop (Eq. (22)) which leads to an increase in the convective term.

Figure 4(b) shows the evolution of L_{th} as a function of Kn for different Péclet numbers with no viscous dissipation and no temperature jump condition. It is verified that L_{th} increases with the increase of the Péclet number similarly to Figs. 2(b) and 3(b). For small Péclet numbers ($Pe_U = 1; 5$), L_{th} is approximately constant while there is a slow decrease as Kn increases for larger Péclet number ($Pe_U = 10$).

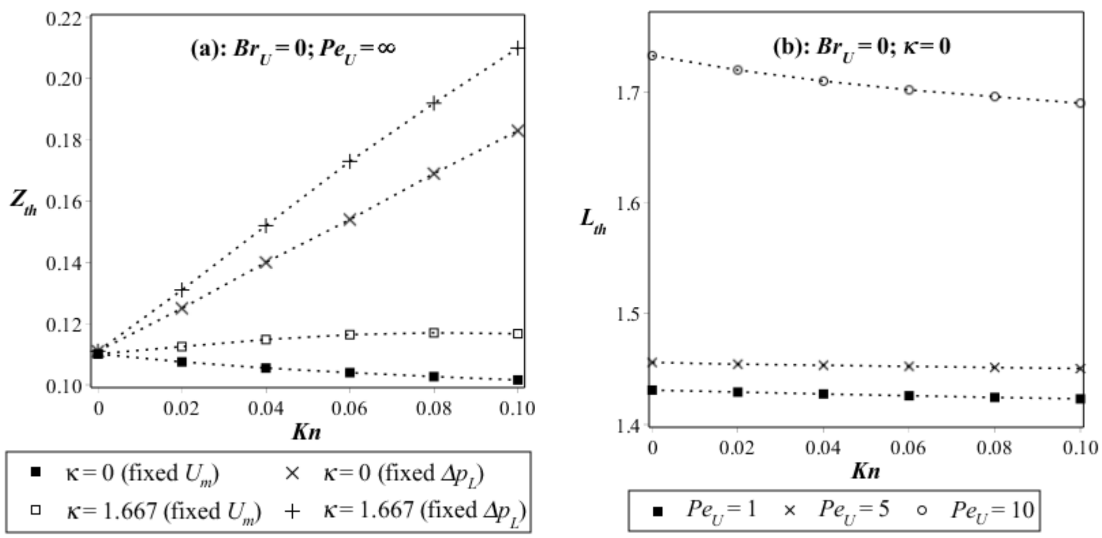

Fig. 4: Evolution of the thermal entrance length as a function of the Knudsen number for different Péclet numbers and degrees of temperature jump with no viscous dissipation.

5. Conclusion

This paper presents an investigation on the effects of the axial heat conduction, viscous dissipation, and slip flow on the thermal entrance length of a laminar forced convection in circular microtubes. The flow is assumed to be steady incompressible and the fluid Newtonian with constant thermophysical properties. The wall boundary conditions are given by the first-order slip-velocity and temperature jump models. The problem is solved analytically by using an exact solution to obtain the velocity and temperature distributions. Furthermore, the Nusselt number is determined in terms of the Péclet number, the Brinkman number, the Knudsen number, and the degree of temperature jump. It is found that the thermal entrance length is approximately compared to the radius $\sim 1.4R$ for small Péclet numbers while it is continuously increasing for large Péclet numbers. Therefore, the thermal entrance region could be too important to be neglected for large Péclet numbers. In the other hand, the thermal entrance length decreases as the absolute value of the Brinkman number increases.

Acknowledgements

This work is done with the financial support of the National Center for Scientific and Technical Research (CNRST).

References

[1] R. K. Shah and A. L. London, *Laminar flow forced convection in ducts*. Academic Press, New York, 1978.

[2] J. Lahjomri and A. Oubarra, “Analytical solution of the Graetz problem with axial conduction,” *J. Heat Transfer*, vol. 121, pp. 1078-1083, 1999. https://doi.org/10.1115/1.2826060
[3] Y. Haddout, A. Oubarra, and J. Lahjomri, “Heat transfer in the slip flow with axial heat conduction in a microchannel with walls having a constant temperature,” *J. Eng. Phys. Thermophys.*, vol. 93, pp. 625-636, 2020. https://doi.org/10.1007/s10891-020-02158-9
[4] M. Shaimi, R. Khatyr, and J. Khalid Naciri, “Analytical solution of the extended Graetz problem in microchannels and microtubes with fixed pressure drop,” *Front. Heat Mass Transf.*, vol. 20, 23, 2023. https://doi.org/10.5098/hmt.20.23
[5] G. Fabbri, “Heat Transfer optimization in corrugated wall channels,” *Int. J. Heat Mass Transfer*, vol. 43, pp. 4299-4310, 2000. https://doi.org/10.1016/S0017-9310(00)00054-5
[6] M. Shaimi, R. Khatyr, and J. Khalid Naciri, “Ansys Fluent automation for fluid flow and heat transfer in corrugated channels,” in *Proceedings of the International Conference on Fluid Flow, Heat and Mass Transfer*, Niagara Falls, Canada, 2022, vol. 9, 206. https://doi.org/10.11159/ffhmt22.206
[7] M. Gad-el-Hak, “The fluid mechanics of microdevices – the Freeman scholar lecture,” *J. Fluids Eng.*, vol. 121, pp. 5-33, 1999. https://doi.org/10.1115/1.2822013